

# Clinicopathologic and Prognostic Study of Primary IgA Nephropathy With Light Chain $\lambda$ Restriction in the Mesangial Deposits



Ji Zhang<sup>1,2,3</sup>, Ziyuan Huang<sup>1,2,3</sup>, Sishi Lin<sup>1,2</sup>, Ya Hu<sup>1,2</sup>, Yan Liang<sup>1,2</sup>, Wenxian Qiu<sup>1,2</sup>, Bo Chen<sup>1,2</sup> and Chaosheng Chen<sup>1,2</sup>

<sup>1</sup>Department of Nephrology, The First Affiliated Hospital of Wenzhou Medical University, Wenzhou, Zhejiang, PR China; and <sup>2</sup>Institute of Chronic Kidney Disease, Wenzhou Medical University, Wenzhou, Zhejiang, PR China

**Introduction:** Primary IgA nephropathy (IgAN) with light chain  $\lambda$  restriction in the mesangial deposits (IgAN- $\lambda$ ) has unique immunofluorescence (IF) features. Nevertheless, its clinicopathology and prognosis are still ambiguous.

**Methods:** From January 2002 to December 2020, the clinical and pathologic data of 3872 patients who were diagnosed with having primary IgAN by renal biopsy in our hospital were reviewed. A total of 187 patients who met the selection criteria for IgAN- $\lambda$  were enrolled to conduct a retrospective single-center study. The selection criteria were that IF features conform to light chain  $\lambda$  restriction in the mesangial deposits. According to age, sex, renal function (estimated glomerular filtration rate [eGFR]), and follow-up time, the control group was constructed with 1:3 matched cases of IgAN. The clinicopathologic and prognostic differences between the 2 groups were analyzed.

**Results:** Compared with that in the IgAN group, the serum fibrinogen level in the IgAN- $\lambda$  group was significantly higher ( $P < 0.001$ ). Furthermore, cluster analysis indicated the different clusters involved in fibrinogen between the IgAN- $\lambda$  and IgAN groups and that fibrinogen is associated with factors reflecting renal function in IgAN- $\lambda$  but proteinuria levels in IgAN. The light chain  $\lambda$  deposit in the mesangium is associated with the formation of crescents in those with IgAN- $\lambda$ , but complement C3 deposition in those with IgAN. Our Kaplan-Meier analysis revealed that the prognosis of the IgAN- $\lambda$  group was significantly worse than that of the IgAN group within  $>6$  years of follow-up ( $P = 0.02$ ). The multi-Cox analysis revealed that the light chain  $\lambda$  restriction in the mesangial deposits was an independent risk factor for poor outcomes (eGFR decreased from the baseline  $\geq 30\%$  continuously or reached end-stage renal disease [ESRD] or died).

**Conclusion:** The prognosis of those with IgAN- $\lambda$  was worse than that of those with IgAN, which may be attributed to the light chain  $\lambda$  restriction in the mesangial deposits inducing a significant systemic inflammation manifested as severe clinical features and frequent crescent.

*Kidney Int Rep* (2022) 7, 776–785; <https://doi.org/10.1016/j.ekir.2022.01.1053>

KEYWORDS: clinicopathology; IgA nephropathy; kidney disease; light chain  $\lambda$ ; prognosis

© 2022 International Society of Nephrology. Published by Elsevier Inc. This is an open access article under the CC BY-NC-ND license (<http://creativecommons.org/licenses/by-nc-nd/4.0/>).

Lai *et al.*<sup>1</sup> in 1986 reported that some IF results of primary IgAN revealed light chain  $\lambda$  restriction in the mesangial deposits (result of light chain  $\kappa$  staining was negative), which was different from common light chain co-dominance. Follow-up studies<sup>2–4</sup> mainly focus on its mechanism. Suen *et al.*<sup>5</sup> and Lai *et al.*<sup>6</sup> speculated

that the negative-charged light chain  $\lambda$  combined with the positive-charged unknown antigen in the kidney tissue led to selective deposition. Later, Lai *et al.*<sup>3</sup> and Orfila *et al.*<sup>7</sup> proposed that unknown specific antigens changed the produced light chain ratio  $\kappa/\lambda$ , resulting in excessive light chain  $\lambda$ . Vitro cell experiments revealed a noticeable difference in the light chain ratio  $\kappa/\lambda$  of IgA produced by stimulated and unstimulated cultured B lymphocytes, which provides strong evidence for this hypothesis. The above-mentioned studies were limited to monoclonal IgA deposition in the mesangium. Nevertheless, IgAN- $\lambda$  was often observed when accompanied by other immunoglobulin deposition. As far as we have known, there are few detailed clinical studies involving light chain  $\lambda$  restriction in the mesangial deposits in this

**Correspondence:** Bo Chen or Chaosheng Chen, Department of Nephrology, The First Affiliated Hospital of Wenzhou Medical University, Nanbaixiang, Ouhai District, Wenzhou 325000, Zhejiang, PR China. E-mails: [tpl@wmu.edu.cn](mailto:tpl@wmu.edu.cn) or [chenchaosheng@wmu.edu.cn](mailto:chenchaosheng@wmu.edu.cn)

<sup>3</sup>JZ and ZH contributed equally to this work.

Received 9 December 2021; revised 14 January 2022; accepted 17 January 2022; published online 26 January 2022

situation. Therefore, the clinicopathologic and prognostic characteristics of IgAN- $\lambda$  remain to be clarified.

This study aimed to find out the clinical significance and value of light chain  $\lambda$  restriction in the mesangial deposits in IgAN, but it is not required to meet the criteria of monoclonal IgA deposition. A retrospective single-center research was conducted to compare the difference between the IgAN- $\lambda$  group and the IgAN group in clinicopathology and prognosis, thus providing a reference for clinical diagnosis and treatment.

## METHODS

### Patient Profiles

From January 2002 to December 2020, the clinical and pathologic data of 3872 patients who were diagnosed with having IgAN by renal biopsy in our hospital were reviewed. A total of 187 patients who met the selection criteria for IgAN- $\lambda$  were enrolled. The selection criteria for IgAN- $\lambda$  were as follows: (i) IgAN was diagnosed by renal biopsy in our hospital and (ii) IF results confirmed light chain  $\lambda$  restriction in the mesangial deposits (the light chain  $\lambda$  staining was equal to or more than + and light chain  $\kappa$  staining was negative). The following patients were excluded: (i) accompanied with other primary or secondary glomerular diseases; (ii) IF results revealed that light chain  $\kappa$  staining was positive; (iii) immunofixation electrophoresis or bone marrow puncture indicated abnormality<sup>8–10</sup>; (iv) clinical data were incomplete; and (v) pathologic diagnosis in our hospital was absent. The clinical and pathologic data of 187 patients who met the above-mentioned criteria were collected. In addition, according to age, sex, renal function (eGFR), and follow-up time, the control group was constructed with 1:3 matched cases of IgAN, and the clinical, pathologic, and prognostic differences between the 2 groups were analyzed. This is a retrospective single-center study. All data were collected from the hospital information system of The First Affiliated Hospital of Wenzhou Medical University, and the Ethics Committee of The First Affiliated Hospital of Wenzhou Medical University approved the protocol for data collection and masking of patient identifiable information.

### Clinical Parameters and Laboratory Data

Variables of sex, age, height (m), weight (kg), blood pressure (mm Hg), hemoglobin (g/l), serum creatinine (s-Cr, mg/dl), serum albumin (g/l), uric acid (mg/dl), blood urea, total cholesterol (mmol/l), triglyceride (mmol/l), high-density lipoprotein—cholesterol (mmol/l), low-density lipoprotein—cholesterol (mmol/l), serum fibrinogen (g/l), serum light chain  $\lambda$  (mg/l), serum light chain  $\kappa$  (mg/l), and 24-hour proteinuria (g/

d) were collected at diagnosis or at the time of first renal biopsy and considered the baseline level. The 24-hour proteinuria level was categorized into 3 according to the tertiles at baseline (low: 0.04–0.92 g/d; medium: 0.93–2.11 g/d; high: 2.12–19.95 g/d). The serum fibrinogen level was categorized into 3 according to the tertiles at baseline (low: 1.07–3.17 g/l; medium: 3.18–4.64 g/l; high: 4.65–10.52 g/l). The eGFR was calculated using the Chronic Kidney Disease Epidemiology Collaboration equation,<sup>11</sup> as follows: male:  $eGFR = 144 \times (s-Cr/0.9)^{-0.411} \times (0.993)^{age}$  ( $s-Cr \leq 0.9$  ml/dl),  $eGFR = 144 \times (s-Cr/0.9)^{-1.209} \times (0.993)^{age}$  ( $s-Cr > 0.9$  ml/dl); female:  $eGFR = 144 \times (s-Cr/0.7)^{-0.329} \times (0.993)^{age}$  ( $s-Cr \leq 0.7$  ml/dl),  $eGFR = 144 \times (s-Cr/0.7)^{-1.209} \times (0.993)^{age}$  ( $s-Cr > 0.7$  ml/dl). The eGFR was translated into 5 stages of chronic kidney disease according to the Kidney Disease Outcomes Quality Initiative guidelines.

### Histopathologic Examination

All the specimens obtained from renal biopsy were examined by light microscopy and IF. Some of the specimens were examined by electron microscopy (EM). For light microscopy, all the specimens were stained with hematoxylin-eosin, periodic acid–Schiff, periodic acid–methenamine silver, and elastic–Masson trichrome. For IF, frozen sections were stained with the direct immunofluorescent method. Samples for EM were fixed with 2.5% glutaraldehyde and processed for regular-transmission EM. The pathologic diagnosis was based on the Oxford pathologic classification (MESTC-score [mesangial hypercellularity/endocapillary hypercellularity/segmental sclerosis/renal tubular lesion/crescent]) criteria, including mesangial hypercellularity (M0/1), endocapillary hypercellularity (E0/1), segmental glomerulosclerosis (S0/S1), tubular atrophy and interstitial fibrosis (T0/1/2), and crescent (C0/1). On the basis of results of light microscopy, statistics were made on the number of glomeruli, global sclerosis, mesangial hypercellularity, mesangial matrix expansion, endocapillary hypercellularity, crescent, adhesion, and so on. On the basis of results of IF, statistics were made on the deposition sites of immunoglobulin (IgG, IgA, IgM), complement (C3, C4), fibrinogen, and light chain ( $\kappa$ ,  $\lambda$ ). The staining intensity was classified into – (not visible in low-power microscopy and not or seems to be visible in high-power microscopy), + (seems to be visible in low-power microscopy and visible in high-power microscopy), ++ (visible in low-power microscopy and clearly visible in high-power microscopy), +++ (clearly visible in low-power microscopy and dazzling in high-power microscopy), and ++++ (dazzling in both low- and high-power microscopy).<sup>12</sup> If the

intensity fluctuates no  $>1$  level, the higher level was chosen to represent the intensity (e.g., + to ++ was scored as ++). If the intensity fluctuates to  $>1$  level, the mean level was chosen to represent the intensity (e.g., + to +++ was scored as ++). The staining intensity of the light chain  $\lambda$  deposit in the mesangium was categorized into 2 levels according to the median (low: +; high: ++ to ++++). On the basis of results of EM, statistics were made on mesangial hypercellularity, mesangial matrix hyperplasia, basement membrane thickening, foot process fusion, and sites of electron-dense deposition.

### Outcomes

The composite end point was defined as (i) eGFR decreased from the baseline  $\geq 30\%$  continuously or (ii) reaching ESRD or (iii) death.

### Statistical Analysis

The variables of age, sex, eGFR, and follow-up time were matched among the IgAN- $\lambda$  and the IgAN groups using the propensity score matching algorithm with a ratio of 1:3. The numerical data are presented as the means (SD) or medians [interquartile range], and differences between groups were evaluated using variance analysis or the Kruskal–Wallis rank test. The categorical data are presented as counts with percentages (%), and differences between groups were analyzed using Pearson's  $\chi^2$  test. Benjamini and Hochberg method was used for correction of multiple comparisons. The correlation coefficient (Pearson for linear data and Kendall for ranked data) was calculated to plot the heatmap. Then, hierarchical clustering<sup>13</sup> was used to perform a network to display the clustering relationship. The adjusted standardized residual was calculated and used to plot the mosaic plot.<sup>14</sup> A multivariable Cox regression model was constructed and optimized using forward-backward stepwise methods and Akaike information criterion. The Kaplan–Meier curve was used to display the end point. All reported *P* values were 2-tailed, and *P* < 0.05 was considered statistically significant. R version 4.0.4 and R packages (such as pheatmap,<sup>15</sup> vcd,<sup>14</sup> and survminer<sup>16</sup>) were used to perform the analyses and plots.<sup>17,18</sup>

## RESULTS

### Clinical Parameters

According to the inclusion and exclusion criteria mentioned previously, a total of 187 patients with IgAN- $\lambda$  were selected from patients who underwent renal biopsy in our hospital from January 2002 to December 2020. The average age of the patients at diagnosis was 39 years old. The maximum age was 78 years old, and the minimum age was 19 years old. The

male-to-female ratio was 1:1.67. Table 1 reveals the differences between the IgAN- $\lambda$  group (right column) and the IgAN group (left column). After matching age, sex, eGFR, and follow-up time, there was no significant difference in demographic data between the 2 groups. The IgAN- $\lambda$  group had significantly more average 24-hour proteinuria (*P* = 0.04), higher average serum fibrinogen level (*P* < 0.001), lower average serum albumin level (*P* < 0.001), higher average uric acid level (*P* = 0.04), higher average total cholesterol level (*P* < 0.001), higher average serum low-density lipoprotein–cholesterol level (*P* = 0.02), lower average serum light chain  $\lambda$  and  $\kappa$  level (*P* < 0.001), and lower  $\kappa/\lambda$  (*P* = 0.01). Patients with IgAN- $\lambda$  got more aggressive treatment, using more steroids (*P* < 0.001), more immunosuppressants (*P* < 0.001), and more angiotensin II receptor blockers (*P* < 0.001). When using eGFR decreased from the baseline  $\geq 30\%$  continuously or reached ESRD or died as the composite end point, a marginal higher proportion of composite end point was observed in the IgAN- $\lambda$  group against the IgAN group (21.4 vs. 15.5%, *P* = 0.09).

The correlation matrix (Figure 1a) and network diagram (Figure 1b) of the clinical parameters of the 2 groups reveal obvious differences in the cluster in which serum fibrinogen level was correlated with between the IgAN- $\lambda$  group and the IgAN group. In the IgAN- $\lambda$  group, the serum fibrinogen level was associated with uric acid level and blood urea level and was most correlated with s-Cr level (Figure 1b). In the IgAN group, the serum fibrinogen level was correlated with total cholesterol and low-density lipoprotein–cholesterol and was most correlated with 24-hour proteinuria level (Figure 1b). The mosaic plot (Figure 1c) reveals that in the IgAN- $\lambda$  group, higher serum fibrinogen level may be associated with worse renal function, and the difference was more evident than that in the IgAN group. In the IgAN group, higher serum fibrinogen levels may be associated with more 24-hour proteinuria, and the difference was more evident than that in the IgAN- $\lambda$  group.

### Renal Pathologic Manifestations

#### Light Microscopy

The results are found in Table 2. In this study, the average number of the glomeruli in the renal biopsy samples was 20.21 and the average number of global sclerosis was 3.84. The IgAN- $\lambda$  group had a significantly higher proportion of mesangial hypercellularity (*P* < 0.001), a higher proportion of endocapillary hypercellularity (*P* = 0.05), a higher proportion of tubular atrophy and interstitial fibrosis (*P* < 0.001), and a higher proportion of crescent

**Table 1.** Baseline comparison of IgAN group and IgAN- $\lambda$  group

Item	IgAN	IgAN- $\lambda$	P value	Adjusted P value
n	561	187		
Male (%)	215 (38.3)	70 (37.4)	0.8	0.8
Age, yr, mean (SD)	38.99 (13.00)	38.53 (12.53)	0.7	0.7
BMI, mean (SD)	23.13 (3.49)	23.09 (3.59)	0.9	1
MBP, mm Hg, mean (SD)	98.17 (13.28)	96.73 (12.33)	0.2	0.3
Follow-up mo, mo, mean (SD)	34.22 (30.83)	35.53 (29.01)	0.6	0.7
Proteinuria, g/d, mean (SD)	1.86 (2.07)	2.29 (2.38)	0.02	0.04
Hematuria, n %	495 (88.2)	173 (92.5)	0.1	0.2
Hemoglobin, g/l, mean (SD)	125.15 (18.43)	124.84 (20.21)	0.8	0.9
Fibrinogen, g/l, mean (SD)	3.47 (1.10)	4.28 (1.34)	<0.001	<0.001
Serum albumin, g/l, mean (SD)	38.01 (7.52)	34.47 (5.96)	<0.001	<0.001
UA, mg/dl, mean (SD)	6.03 (1.64)	6.36 (1.71)	0.02	0.04
BU, mean (SD)	5.89 (2.71)	6.16 (2.82)	0.2	0.4
Serum creatinine, mg/dl, mean (SD)	1.12 (1.02)	1.09 (0.70)	0.7	0.7
eGFR, ml/min per 1.73 m <sup>2</sup> , mean (SD)	91.36 (32.03)	91.19 (35.56)	0.9	1
Total cholesterol, mmol/l, mean (SD)	4.88 (1.40)	5.38 (1.68)	<0.001	<0.001
Triglyceride, mmol/l, mean (SD)	1.85 (1.21)	1.96 (1.44)	0.3	0.5
HDL, mmol/l, mean (SD)	1.12 (0.29)	1.17 (0.33)	0.08	0.1
LDL, mmol/l, mean (SD)	2.88 (1.04)	3.13 (1.27)	0.008	0.02
Serum light chain $\kappa$ , mg/l, mean (SD)	8.60 (2.92)	6.94 (2.99)	<0.001	<0.001
Serum light chain $\lambda$ , mg/l, mean (SD)	4.64 (1.61)	3.94 (1.70)	<0.001	<0.001
$\kappa/\lambda$ , mean (SD)	1.89 (0.37)	1.80 (0.36)	0.004	0.01
Nephrotic syndrome, n (%)	31 (5.5)	25 (13.4)	0.001	0.002
End point, n (%)	87 (15.5)	40 (21.4)	0.08	0.09
Steroid, n (%)	161 (28.7)	83 (44.4)	<0.001	<0.001
ACEI, n (%)	93 (16.6)	26 (13.9)	0.5	0.6
ARB, n (%)	286 (51.0)	150 (80.2)	<0.001	<0.001
CTX, n (%)	12 (2.1)	7 (3.7)	0.3	0.5
Other IM = 1, n (%)	39 (7.0)	35 (18.7)	<0.001	<0.001
Steroid use duration, mo, mean (SD)	1.04 (2.53)	4.28 (10.65)	<0.001	<0.001
IM use duration, mo, mean (SD)	0.67 (3.39)	2.89 (10.61)	<0.001	<0.001

ACEI, angiotensin-converting enzyme inhibitor; ARB, angiotensin receptor blocker; BMI, body mass index; BU, blood urea; CTX, cyclophosphamide; eGFR, estimated glomerular filtration rate; HDL, high-density lipoprotein; IgAN- $\lambda$ , primary IgA nephropathy with light chain  $\lambda$  restriction in the mesangial deposits; IgAN, primary IgA nephropathy; IM, immunosuppressant; LDL, low-density lipoprotein; MBP, mean blood pressure; UA, uric acid.

All data were acquired before the renal biopsy.

formation ( $P < 0.001$ ). In the IgAN- $\lambda$  group, the crescents appeared in 93 cases, mostly small crescents, including 56 cases of the cellular crescent, 54 cases of the fibrocellular crescent, and 38 cases of the fibrous crescent. The proportion of fibrocellular crescent is higher ( $P = 0.02$ ). The proportion of capillary loop necrosis was higher ( $P < 0.001$ ). Most patients had renal interstitial inflammation, revealing interstitial lymphocyte and plasma cell infiltration, renal tubular atrophy, and renal interstitial fibrosis. A total of 8 cases accompanied acute interstitial inflammation, including 7 cases of mild inflammation and 1 case of moderate inflammation. In addition, 177 cases accompanied chronic interstitial inflammation, including 103 cases of mild inflammation, 58 cases of moderate inflammation, and 16 cases of severe inflammation. Most patients had varying degrees of vascular lesions, including mild endarterium hyperplasia in 64 cases, moderate endarterium hyperplasia in 25 cases, severe endarterium

hyperplasia in 11 cases, and a higher proportion of hyalinosis ( $P = 0.05$ ).

### Immunofluorescence

The results are found in Table 3. The fluorescent tissue contains an average of 4.42 glomeruli (2–15 glomeruli). IgA is the dominant or co-dominant immunoglobulin deposited in the glomeruli (intensity + to ++++). The mode of deposition is coarse granular or massive in the glomerular mesangial area and/or capillary wall. In the IgAN- $\lambda$  group, the deposition rate of IgA in the capillary wall was 4.3%, which was significantly higher than the IgAN group ( $P = 0.01$ ) with higher staining intensity ( $P = 0.02$ ). Of the cases, 93% had C3 deposition in the mesangial area, of which the proportion is significantly higher ( $P = 0.04$ ), and 2.7% in the capillary wall. The deposition rates of IgG and IgM in the mesangial area and capillary wall were 7.5%, 1.0% and 39.6%, 2.7%, respectively, which were not significantly different from those in the IgAN group.

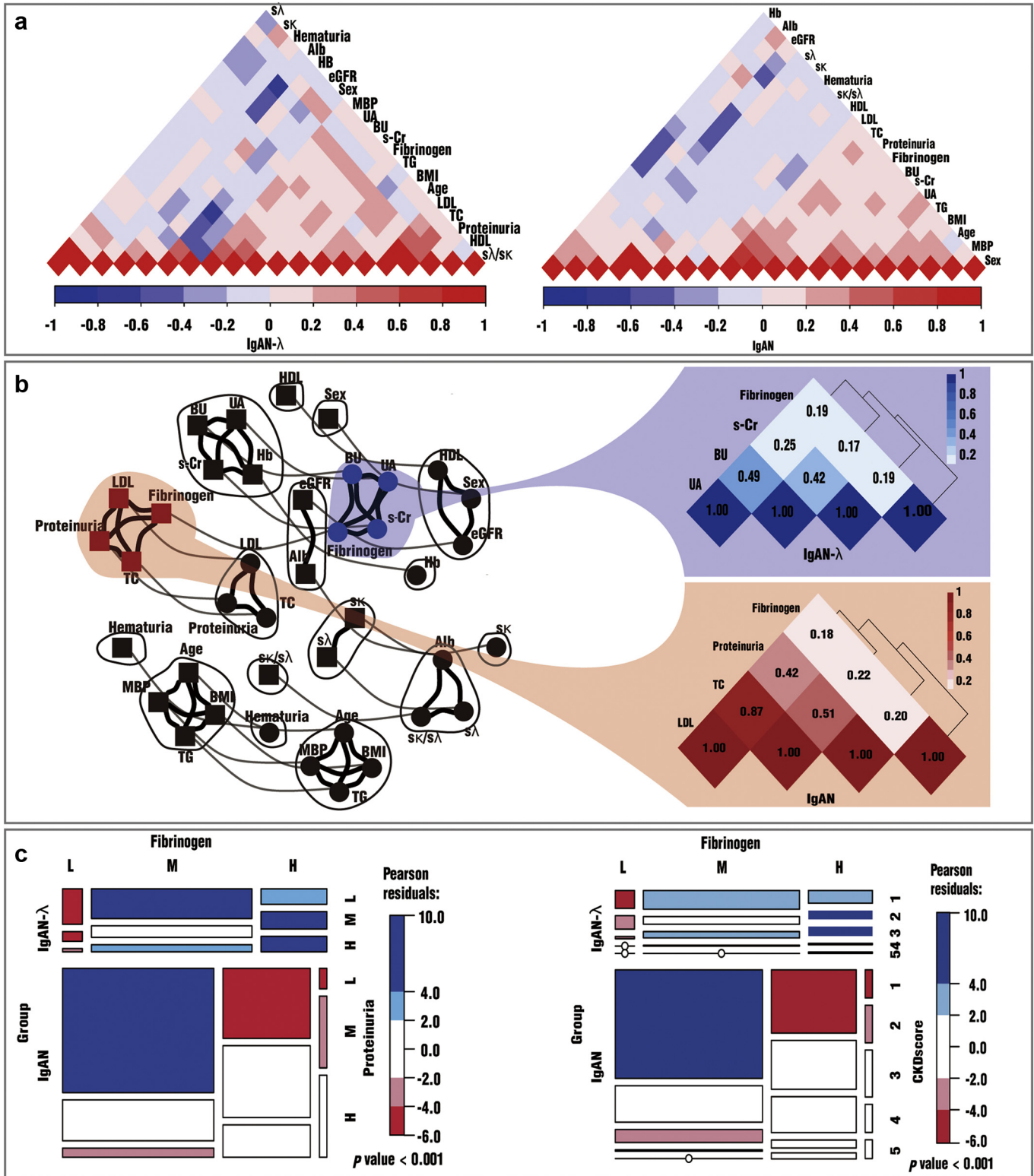


**Figure 1.** Cluster analysis for clinical factors between the groups. (a) The heatmaps display the correlation coefficient (Pearson’s correlation coefficient for linear data) of the clinical factors in IgAN- $\lambda$  and IgAN. The color label under the heatmap reveals that the red shade represents a positive correlation whereas the blue shade represents a negative correlation. The related factors shared the same or similar colors. (b) The network diagram displays the clinical factors’ clustering relationship in IgAN- $\lambda$  and IgAN. The nodes represent the factors, and the shapes of the nodes represent the groups (circle for IgAN- $\lambda$  and square for IgAN). The nodes connected by a solid black line reveal a stronger correlation and construct a cluster whereas the nodes connected by the solid gray line are the same factors from the different groups (the same factors are assigned a tiny weight, and different factors are assigned the same larger weight). The clusters, including the factor “Fibrinogen” of the 2 groups, are chosen to make cluster analysis by using the heatmap. (c) The mosaic plots display the relationships between levels of fibrinogen and CKD score/proteinuria levels in the 2 groups. The size of boxes is proportional to the frequency of each item. The shadings are (continued)

All cases were negative for light chain  $\kappa$  staining (Supplementary Figure S1) and positive for light chain  $\lambda$  staining (intensity + to ++++). The proportion of light chain  $\lambda$  deposition in the capillary wall was 5.8%, which was significantly higher than that in the IgAN group ( $P < 0.001$ ).

### Electron Microscopy

The results are found in Supplementary S1. Of the 187 patients with IgAN- $\lambda$ , 94 were examined by EM. Ultrastructurally, the deposition rate of electronic dense in the mesangial area was 69.1%, which was lower than that in the IgAN group ( $P < 0.001$ ). The deposition rate of electronic dense in the paramesangial area was 41.5% higher than that in the IgAN group ( $P < 0.001$ ). Furthermore, of the cases, the deposition was 6.4% in the subepithelial and 3.2% in the subendothelial. Most patients had foot process fusion. There were 42.6% of the cases who had diffuse foot process fusion, which was higher than the IgAN group ( $P = 0.004$ ), and 48.9% of the cases had segmental foot process fusion. Some patients had thickened basement membrane, including 8 cases with mild thickening and 2 cases with moderate thickening.

The correlation matrix (Supplementary Figure S2A) and network diagram (Supplementary Figure S2B) of the pathologic parameters of the 2 groups reveal obvious differences in the cluster in which light chain  $\lambda$  deposit in the mesangium was correlated with between the IgAN- $\lambda$  and the IgAN groups. In the IgAN- $\lambda$  group, the light chain  $\lambda$  deposit in the mesangium was correlated with chronic inflammation in the renal interstitium, T1, and capillary loop necrosis and most correlated with C1 (Supplementary Figure S2B). Nevertheless, in the IgAN group, the light chain  $\lambda$  deposit in the mesangium was correlated with the IgA deposit in the mesangium and most correlated with the C3 deposit in the mesangium (Supplementary Figure S2B). The mosaic plot revealed that a high level of light chain  $\lambda$  deposit in the mesangium was significantly associated with a higher C-score and C3 deposition, either in the IgAN- $\lambda$  or the IgAN group. Furthermore, the IgAN- $\lambda$  group has an increasingly high level of light chain  $\lambda$  deposit in the mesangium. It is associated with a significantly increased crescent formation and C3 deposition proportion (Supplementary Figure S2C).

**Table 2.** Light microscopy result comparison of IgAN group and IgAN- $\lambda$  group

Item	IgAN	IgAN- $\lambda$	P value	Adjusted P value
Number of glomeruli, mean (SD)	20.16 (11.20)	20.39 (10.58)	0.8	0.8
Global sclerosis, mean (SD)	3.70 (4.28)	4.25 (4.12)	0.1	0.2
M1, n (%)	147 (26.2)	81 (43.3)	<0.001	<0.001
E1, n (%)	155 (27.6)	67 (35.8)	0.04	0.05
S1, n (%)	338 (60.2)	118 (63.1)	0.5	0.7
T-score, n (%)			<0.001	<0.001
T0	431 (76.8)	113 (60.8)		
T1	97 (17.3)	49 (26.3)		
T2	33 (5.9)	24 (12.9)		
C1, n (%)	59 (10.5)	93 (49.7)	<0.001	<0.001
Mesangial hypercellularity, n (%)	490 (87.3)	174 (93.0)	0.02	<0.001
Mesangial matrix expansion, n (%)	497 (88.6)	178 (95.2)	0.007	0.01
Endocapillary hypercellularity, n (%)	141 (25.1)	66 (35.3)	0.009	0.02
Adhesion, n (%)	372 (66.3)	120 (64.2)	0.7	0.7
Cases with crescents, n (%)				
Cellular crescent	138 (24.6)	56 (29.9)	0.2	0.3
Fibrocellular crescent	108 (19.3)	54 (28.9)	0.008	0.02
Fibrous crescent	88 (15.7)	38 (20.3)	0.2	0.3
Interstitial inflammation change, n (%)				
Acute-mild inflammation	7 (1.2)	7 (3.7)	0.06	0.1
Acute-moderate inflammation	8 (1.4)	1 (0.5)	0.6	0.7
Acute-severe inflammation	0 (0.0)	0 (0.0)	—	—
Chronic-mild inflammation	327 (58.3)	103 (55.1)	0.5	0.7
Chronic-moderate inflammation	99 (17.6)	58 (31.0)	<0.001	<0.001
Chronic-severe inflammation	51 (9.1)	16 (8.6)	0.9	1
Vasculopathy, n (%)				
Mild endarterium hyperplasia	152 (27.1)	64 (34.2)	0.07	0.1
Moderate endarterium hyperplasia	37 (6.6)	25 (13.4)	0.006	0.02
Severe endarterium hyperplasia	15 (2.7)	11 (5.9)	0.07	0.1
Hyalinosis	186 (33.2)	80 (42.8)	0.02	0.05
Glomerular capillary loop necrosis	33(5.9)	34(20.9)	<0.001	<0.001

C1, crescents in at least 1 glomerulus; E1, endocapillary hypercellularity; IgAN- $\lambda$ , primary IgA nephropathy with light chain  $\lambda$  restriction in the mesangial deposits; IgAN, primary IgA nephropathy; M1, mesangial hypercellularity; S1, segmental glomerulosclerosis; T1/2, tubular atrophy and interstitial fibrosis.

### Prognosis and Risk Factors

The average follow-up time was 34.56 months (2–100 months). When eGFR decreased from the

**Figure 1.** (continued) made based on the Pearson residuals that were calculated by the R package of vcd. The blue shades represent high residuals whereas red shades mean the opposite. Alb, serum albumin; BMI, body mass index; BU, blood urea; CKD, chronic kidney disease; eGFR, estimated glomerular filtration rate; H, high; Hb, hemoglobin; HDL, high-density lipoprotein; IgAN- $\lambda$ , IgAN with light chain  $\lambda$  restriction in the mesangial deposits; IgAN, primary IgA nephropathy; L, low; LDL, low-density lipoprotein; M, medium; MBP, mean blood pressure; s-Cr, serum creatinine; s $\kappa$ , serum light chain  $\kappa$ ; s $\lambda$ , serum light chain  $\lambda$ ; TC, total cholesterol; TG, triglyceride; UA, uric acid.

**Table 3.** Immunofluorescence result comparison of IgAN group and IgAN- $\lambda$  group

Item	IgAN	IgAN- $\lambda$	P value	Adjusted P value
Deposit site, n (%)				
IgA in capillary wall	7(1.3)	8(4.3)	0.008	0.01
IgA in mesangium	561(100)	187(100)	0.4	0.67
IgM in capillary wall	34(6.1)	5(2.7)	0.3	0.4
IgM in mesangium	261(46.5)	74(39.6)	0.1	0.2
IgG in capillary wall	5(0.9)	2(1)	0.7	0.7
IgG in mesangium	51(9.1)	14(7.5)	0.3	0.4
C3 in capillary wall	13(2.3)	5(2.7)	0.8	1
C3 in mesangium	482(86.0)	174(93.0)	0.01	0.04
C4 in mesangium	0(0.0)	3(1.6)	0.01	0.04
Fibrinogen in capillary wall	23(4.1)	1(0.5)	0.03	0.05
Fibrinogen in mesangium	101(18.0)	21(11.2)	0.004	0.005
$\kappa$ in capillary wall	4 (0.7)	0 (0.0)	0.6	0.7
$\kappa$ in mesangium	367(65.4)	0(0.0)	<0.001	<0.001
$\lambda$ in capillary wall	2(0.4)	11(5.8)	<0.001	<0.001
$\lambda$ in mesangium	368(65.1)	187(100)	<0.001	<0.001
Intensity score				
	1/2/3/4 (median)	1/2/3/4 (median)		
IgA in capillary wall	0/2/5/0 (3)	0/4/2/2 (3.5)	0.01	0.02
IgA in mesangium	9/85/44/9/14 (3)	1/31/14/4/8 (3)	0.9	1
IgM in capillary wall	23/10/1/0 (2)	3/2/0/0 (1)	0.07	0.09
IgM in mesangium	196/60/5/0 (1)	38/14/2/0 (1)	0.09	0.1
IgG in capillary wall	4/1/0/0 (1)	1/1/0/0 (1.5)	0.8	0.8
IgG in mesangium	32/17/2/0 (1)	5/8/1/0 (2)	0.6	0.8
C3 in capillary wall	2/8/3/0 (2)	1/2/2/0 (2)	0.8	0.9
C3 in mesangium	82/204/194/2 (2)	18/87/69/0 (2)	0.04	0.05
C4 in mesangium	0/0/0/0 (0)	2/0/1/0 (1)	0.003	0.006
Fibrinogen in capillary wall	16/7/0/0 (1)	0/1/0/0 (1)	0.02	0.05
Fibrinogen in mesangium	52/42/3/4 (1)	4/12/5/0 (2)	0.07	0.09
$\kappa$ in capillary wall	4/0/0/0 (1)	0/0/0/0 (0)	0.2	0.4

C, crescent; IF, immunofluorescence; IgAN- $\lambda$ , primary IgA nephropathy with light chain  $\lambda$  restriction in the mesangial deposits; IgAN, primary IgA nephropathy.

The intensity of IF was classified as -,  $\pm$ , +, ++, +++, and +++++. An intensity no less than + was defined as positive. If the intensity fluctuates no >1 level, the higher level was chosen to represent the intensity (e.g., + to ++ was scored as ++). If the intensity fluctuates >1 level, the mean level was chosen to represent the intensity (e.g., + to +++ was scored as ++). The intensity score 1/2/3/4 represents +, ++, +++, and +++++, respectively, and the count of each score was found in the table. The  $\chi^2$  test was used for intergroup comparison of deposit sites. Wilcoxon ranked sum test was used for intergroup comparison of the intensity score.

baseline  $\geq 30\%$  continuously or ESRD was reached or death as the composite end point, the prognosis of the IgAN- $\lambda$  group was worse than that of the IgAN group ( $P = 0.02$ ) (Figure 2). Using eGFR decreased from the baseline  $\geq 30\%$  continuously or reaching ESRD or died as the composite end point, univariate Cox regression analysis was performed on the related factors of IgAN- $\lambda$  (Supplementary S2). The results of multivariable Cox regression are found in Table 4. The increased serum albumin level was an independent protective factor ( $P < 0.001$ ), and the increased mean blood pressure ( $P < 0.001$ ), increased s-Cr level ( $P < 0.001$ ), light chain  $\lambda$  restriction in the mesangial deposits ( $P = 0.04$ ), higher staining intensity of light chain  $\lambda$  deposit in the mesangium ( $P = 0.04$ ), renal tubular atrophy or interstitial fibrosis ( $P < 0.001$ ), increased 24-hour proteinuria ( $P = 0.01$ ), increased serum fibrinogen

level ( $P = 0.02$ ), and increased triglyceride level ( $P = 0.006$ ) were independent risk factors.

The mosaic plot reveals that higher serum fibrinogen levels in both groups may be associated with a worse prognosis (Supplementary Figure S3). In the middle/high level of the fibrinogen group, the difference in the IgAN- $\lambda$  group is more obvious than that in the IgAN group. Higher staining intensity of light chain  $\lambda$  deposit may be associated with worse prognosis in the IgAN- $\lambda$  group (Supplementary Figure S3). In the high staining intensity of the light chain  $\lambda$  group, the difference in the IgAN group is more obvious than in the IgAN- $\lambda$  group. For the IgAN- $\lambda$  group, in the high-level fibrinogen group and low staining intensity of the light chain  $\lambda$  group, the prognosis of those with immunosuppressant + steroid therapy was poorer, and the differences were obvious (Supplementary Figure S3).

## DISCUSSION

Our study revealed that the IgAN- $\lambda$  group had significantly higher serum fibrinogen levels than the IgAN group. The cluster analysis found that the serum fibrinogen level correlated with different clusters in the 2 groups, suggesting the inflammation may have different meanings. In the IgAN- $\lambda$  group, the serum fibrinogen level was correlated with renal function indicators, especially the s-Cr level. Higher serum fibrinogen levels were associated with more severe deterioration of renal function, indicating the inflammation destroyed the structure and function of the kidney more directly. In the IgAN group, however, serum fibrinogen level was correlated with the indicators related to nephrotic syndrome, especially 24-hour proteinuria. As far as we have known, nephrotic syndrome may be the early stage of renal failure, which suggests that the IgAN- $\lambda$  group progressed faster than the IgAN group and got more severe inflammation. Lai *et al.*<sup>19</sup> found through experiments that the monoclonal light chain  $\lambda$  of IgA could further activate leukocytes to undergo chemotaxis and aggregation after the initial binding of leukocytes. Aggregated leukocytes caused inflammatory damage. On one hand, it caused the increase of serum fibrinogen levels, and on the other hand, it participated in the damage of the glomerular interstitium, which may lead to renal failure, which is consistent with our results. Previous studies proposed that patients with IgAN- $\lambda$  relatively rarely progress to chronic kidney disease, and the probability of acute disease was not significantly different from patients with IgAN, but our study suggested that the lesions were more severe, which may not support the view.

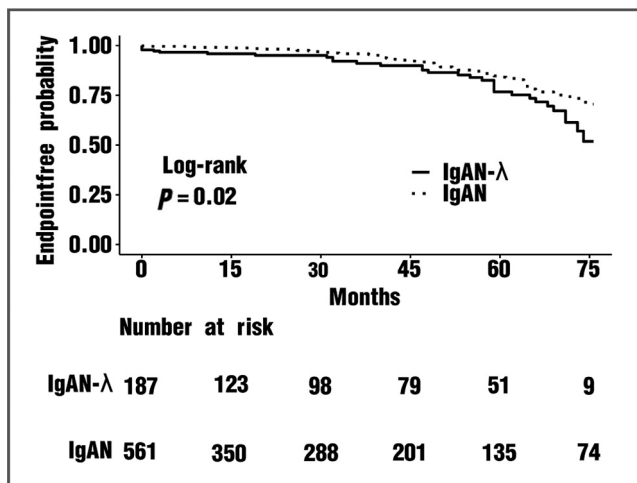


**Figure 2.** Comparison of prognosis between IgAN group and IgAN- $\lambda$  group (Kaplan–Meier curve),  $P = 0.02$  (log-rank test). The end point is the eGFR 30% decrease of the baseline or reaching end-stage renal disease or death. e-GFR, estimated glomerular filtration rate; IgAN- $\lambda$ , IgAN with light chain  $\lambda$  restriction in the mesangial deposits; IgAN, primary IgA nephropathy.

Few reports involve the pathology of IgAN- $\lambda$  except the light chain deposition characteristics. The cluster analysis found that the light chain  $\lambda$  deposit in the mesangium correlated with different clusters in the 2 groups, suggesting the deposit may have different meanings. In the IgAN- $\lambda$  group, the light chain  $\lambda$  deposit in the mesangium was correlated with crescent formation, renal tubulointerstitial atrophy/sclerosis, and chronic interstitial inflammation. As far as we have known, macromolecular proteins such as the fibrinogen could enter the Bowman's capsule through the

**Table 4.** Factors at first kidney biopsy associated with reaching the composite end point

Factors	HR (95% CI for HR)	P value
Clinical factors		
10 mm Hg increase in MBP	1.28 (1.12–1.48)	<0.001
Increased proteinuria (g/d)	1.12 (1.03–1.23)	0.01
Increased s-Cr (mg/dl)	1.30 (1.18–1.44)	<0.001
Increased Alb (g/l)	0.93 (0.91–0.97)	<0.001
Increased TG (mmol/l)	1.21 (1.05–1.38)	0.006
Increased fibrinogen (g/l)	1.06 (1.02–1.10)	0.02
Increased s- $\kappa$ (mg/l)	0.71 (0.70–0.90)	0.1
Increased s- $\lambda$ (mg/l)	1.35 (1.32–1.68)	0.09
Pathologic factors		
Light chain $\lambda$ restriction in the mesangial deposits	1.54 (1.03–2.31)	0.03
T1/T2	5.05 (3.24–7.89)	<0.001
Light chain $\lambda$ intensity	1.34 (1.32–1.36)	0.04

AIC, Akaike information criterion; Alb, serum albumin; eGFR, estimated glomerular filtration rate; HR, hazard ratio; MBP, mean blood pressure; s-Cr, serum creatinine; s- $\kappa$ , serum light chain  $\kappa$ ; s- $\lambda$ , serum light chain  $\lambda$ ; T1/T2, tubular atrophy and interstitial fibrosis; TG, triglyceride.

This is the result of multivariable Cox regression model. The composite end point is the decrease of eGFR to >30% of the baseline or end-stage renal disease or reaching the end-stage renal disease or died. Factors with statistical differences ( $P < 0.1$ ) in univariable Cox regression (as found in [Supplementary S2](#)) or considered meaningful in the cluster analysis were selected to build a multivariable Cox regression model. Then, the AIC using the forward-backward stepwise was performed to select the optimal model with the lowest AIC value. All the data were acquired before the renal biopsy.

damaged capillary loops leading to blood coagulation, monocyte infiltration, secretion of epithelial growth factor, and crescent formation. Our study found that the IgAN- $\lambda$  group was more intended to form crescents (C1 accounted for a higher proportion) and had a higher proportion of capillary loop necrosis. Thus, the pathologic manifestations could further illustrate that the IgAN- $\lambda$  group had more severe inflammation and renal structure damage, which may be associated with the light chain  $\lambda$  deposit in the mesangium. A higher proportion of renal tubulointerstitial atrophy/sclerosis and chronic interstitial inflammation also suggested a step further from the trend of entering chronic kidney disease.

Meanwhile, higher staining intensity led to a higher proportion of crescent formation, indicating a poor prognosis. In the IgAN group, the light chain  $\lambda$  deposit in the mesangium was correlated with C3 and IgA deposit in the mesangium, suggesting the relation to classic immune-mediated inflammation. Setoguchi *et al.*<sup>20</sup> reported a case of IgAN- $\lambda$  whose EM results revealed that the electronic dense was mainly deposited in the mesangium and subendothelium and thought that there were no characteristic structures. Our study found that except for more severe mesangial hypercellularity and a more severe degree of foot process fusion, patients with IgAN- $\lambda$  had a higher proportion of electron-dense deposits in the para-mesangium than those with IgAN. This may relate to the light chain  $\lambda$  restriction mechanism in the mesangial deposits, which needs further study.

Previous studies<sup>21–25</sup> proposed no significant difference in prognosis between patients with IgAN- $\lambda$  and patients with IgAN. Nevertheless, the small sample size and short follow-up time may affect the power of tests and the conclusion. Similarly, our  $\chi^2$  test results revealed a marginal difference in the proportion of composite end points between the IgAN- $\lambda$  and the IgAN groups (21.4 vs. 15.5%,  $P = 0.09$ ). Nevertheless, the Kaplan–Meier analysis displayed a significantly decreased survival rate free from composite end points in the IgAN- $\lambda$  group (log-rank,  $P = 0.02$ ), which strongly indicated a poor prognosis in the IgAN- $\lambda$  group. Furthermore, we found that higher mean blood pressure, more 24-hour proteinuria, higher triglyceride level, higher serum fibrinogen level, and worse renal function at diagnosis resulted in a poorer prognosis. This suggested that patients with hypertension, hyperlipidemia, inflammation, and renal insufficiency should be treated more aggressively. The prognostic difference caused by increased serum fibrinogen level is more obvious in the IgAN- $\lambda$  group, especially in the high-level fibrinogen group, which indicated further that the inflammation destruction may be a cascade. It



also suggested that timely suppression of the inflammatory response and reducing the destruction of the kidney structure may be the key to therapy. The prognostic difference caused by the increased staining intensity of light chain  $\lambda$  deposit in the mesangium is more obvious in the IgAN- $\lambda$  group, suggesting the staining intensity could be used to evaluate the prognosis.

In the high-level fibrinogen group, the steroid + immunosuppressive therapy resulted in an obvious poorer prognosis, which is supposed to be related to the serious condition of these patients at the beginning of treatment, and immunosuppressive therapy may not slow down the progression of the kidneys among these patients. Other effective treatment needs to be further studied. For patients with low staining intensity of light chain  $\lambda$ , the prognosis of steroid + immunosuppressive was obviously poorer than other therapies, which was different from the high staining intensity of the light chain  $\lambda$  group. It suggested that aggressive treatment may be related to poor prognosis for patients with nonserious renal pathologic manifestations, which requires further prospective studies.

Previous studies thought that the clinical significance of light chain  $\lambda$  restriction in the mesangial deposits in IgAN was still controversial, but our present study found it of great value. The research aimed to initially explore the impact of light chain  $\lambda$  restriction in the mesangial deposits on the clinicopathology and prognosis of IgAN. Nevertheless, this research was a single-center retrospective study. Further large-sample and multicenter research are needed.

## CONCLUSION

Compared with patients with IgAN, those with IgAN- $\lambda$  had significantly higher serum fibrinogen levels which correlated with renal function. Pathologic manifestation included a higher proportion of crescent formation, which correlated with light chain  $\lambda$  deposit in the mesangium. The prognosis of IgAN- $\lambda$  was significantly worse than that of IgAN.

## DISCLOSURE

All the authors declared no competing interests.

## ACKNOWLEDGMENTS

The authors thank their colleagues at the Department of Nephrology, The First Affiliated Hospital of Wenzhou Medical University, for their support and assistance during the study period. This work was supported by a grant from the Natural Science Foundation of Zhejiang Province (No. LY22H050004).

## ETHICS APPROVAL AND CONSENT TO PARTICIPATE

This retrospective study has complied with the guidelines of the Declaration of Helsinki and was approved by the Medical Ethics Committee of The First Affiliated Hospital of Wenzhou Medical University, Wenzhou, Zhejiang. Because this study involved a retrospective review of existing data, approval from the Institutional Review Board was obtained, and administrative permissions were not required. There was no specific, informed consent from the patients. The Institutional Review Board of The First Affiliated Hospital of Wenzhou Medical University specifically waived the need for consent for these studies.

## AVAILABILITY OF DATA AND MATERIALS

The data sets used and/or analyzed in this study are available from the corresponding author on reasonable request.

## AUTHOR CONTRIBUTIONS

JZ and ZH collected the clinical and pathologic data and analyzed and drafted the manuscript. SL, YH, YL, WQ acquired the data and material support. BC and CC contributed to the conception and design. BC analyzed and interpreted the data. BC and CC revised the manuscript. CC supervised the study, provided the project funding, and finally approved the version of the manuscript for publication.

## SUPPLEMENTARY MATERIAL

Supplementary File (PDF)

**Supplementary S1.** Electron microscopy result comparison of IgAN group and IgAN- $\lambda$  group.

**Supplementary S2.** Univariable analysis for factors associated with the composite end point.

**Figure S1.** Pathologic manifestations for IgAN- $\lambda$  group.

**Figure S2.** Cluster analysis for pathologic factors between groups.

**Figure S3.** Mosaic plots displaying the relationships between factors.

**STROBE Statement.**

## REFERENCES

1. Lai KN, Chan KW, Mac-Moune F, et al. The immunochemical characterization of the light chains in the mesangial IgA deposits in IgA nephropathy. *Am J Clin Pathol.* 1986;85:548–551. <https://doi.org/10.1093/ajcp/85.5.548>
2. Lai KN, Lai FM, Lo ST, Lam CW. Light chain composition of IgA in IgA nephropathy. *Am J Kidney Dis.* 1988;11:425–429. [https://doi.org/10.1016/s0272-6386\(88\)80056-8](https://doi.org/10.1016/s0272-6386(88)80056-8)
3. Lai KN, Chui SH, Lai FM, Lam CW. Predominant synthesis of IgA with lambda light chain in IgA nephropathy. *Kidney Int.* 1988;33:584–589. <https://doi.org/10.1038/ki.1988.37>

4. Jennette JC. The immunohistology of IgA nephropathy. *Am J Kidney Dis.* 1988;12:348–352. [https://doi.org/10.1016/s0272-6386\(88\)80022-2](https://doi.org/10.1016/s0272-6386(88)80022-2)
5. Suen KK, Lewis WH, Lai KN. Analysis of charge distribution of lambda- and kappa-IgA in IgA nephropathy by focused antigen capture immunoassay. *Scand J Urol Nephrol.* 1997;31:289–293. <https://doi.org/10.3109/00365599709070350>
6. Lai KN, Chui SH, Lewis WH, et al. Charge distribution of IgA-lambda in IgA nephropathy. *Nephron.* 1994;66:38–44. <https://doi.org/10.1159/000187763>
7. Orfila C, Rakotoarivony J, Manuel Y, Suc JM. Immunofluorescence characterization of light chains in human nephropathies. *Virchows Arch A Pathol Anat Histopathol.* 1988;412:591–594. <https://doi.org/10.1007/BF00844295>
8. Sumida K, Ubara Y, Marui Y, et al. Recurrent proliferative glomerulonephritis with monoclonal IgG deposits of IgG2 $\lambda$  subtype in a transplanted kidney: a case report. *Am J Kidney Dis.* 2013;62:587–590. <https://doi.org/10.1053/j.ajkd.2013.01.013>
9. Nasr SH, Sethi S, Cornell LD, et al. Proliferative glomerulonephritis with monoclonal IgG deposits recurs in the allograft. *Clin J Am Soc Nephrol.* 2011;6:122–132. <https://doi.org/10.2215/CJN.05750710>
10. Albawardi A, Satoskar A, Von Visger J, Brodsky S, Nadasdy G, Nadasdy T. Proliferative glomerulonephritis with monoclonal IgG deposits recurs or may develop de novo in kidney allografts. *Am J Kidney Dis.* 2011;58:276–281. <https://doi.org/10.1053/j.ajkd.2011.05.003>
11. Ahmed S, Jafri L, Khan AH. Evaluation of ‘CKD-EPI Pakistan’ equation for estimated glomerular filtration rate (eGFR): A comparison of eGFR prediction equations in Pakistani population. *J Coll Phys Surg Pak.* 2017;27:414–418.
12. Kazi AM, Hashmi MF. Glomerulonephritis. In: *StatPearls*. StatPearls Publishing LLC; 2021.
13. Wang Y, Ye Y, Li X, et al. Hierarchical information-theoretic co-clustering for high dimensional data. *Int J Innov Comput Inf Control.* 2011;7:487–500.
14. Friendly M. ‘vcd’ Extensions and Additions [R package vcdExtra version 0.7-1]. 2015.
15. Gu Z, Huebschmann D. Make interactive complex heatmaps in R. *Bioinformatics.* 2022;38:1460–1462.
16. Kassambara A. *Drawing Survival Curves Using ‘ggplot2’ [R Package Survminer Version 0.2.0]*. 2017.
17. Ginestet C. ggplot2: elegant graphics for data analysis. *J R Stat Soc A.* 2011;174, 245–245.
18. Dean CB, Nielsen JD. Generalized linear mixed models: a review and some extensions. *Lifetime Data Anal.* 2007;13:497–512. <https://doi.org/10.1007/s10985-007-9065-x>
19. Lai KN, Chan LY, Tang SC, et al. Characteristics of polymeric lambda-IgA binding to leukocytes in IgA nephropathy. *J Am Soc Nephrol.* 2002;13:2309–2319. <https://doi.org/10.1097/01.asn.0000026497.82930.73>
20. Setoguchi K, Kawashima Y, Tokumoto T, et al. Proliferative glomerulonephritis with monoclonal immunoglobulin A light-chain deposits in the renal allograft. *Nephrol (Carlton).* 2014;19(suppl 3):49–51. <https://doi.org/10.1111/nep.12251>
21. Wu L, Liu D, Xia M, et al. Immunofluorescence deposits in the mesangial area and glomerular capillary loops did not affect the prognosis of immunoglobulin A nephropathy except C1q: a single-center retrospective study. *BMC Nephrol.* 2021;22:43. <https://doi.org/10.1186/s12882-021-02237-w>
22. Nagae H, Tsuchimoto A, Tsuruya K, et al. Clinicopathological significance of monoclonal IgA deposition in patients with IgA nephropathy. *Clin Exp Nephrol.* 2017;21:266–274. <https://doi.org/10.1007/s10157-016-1275-7>
23. Alpers CE, Tu WH, Hopper J Jr, Biava CG. Single light chain subclass (kappa chain) immunoglobulin deposition in glomerulonephritis. *Hum Pathol.* 1985;16:294–304. [https://doi.org/10.1016/s0046-8177\(85\)80017-4](https://doi.org/10.1016/s0046-8177(85)80017-4)
24. Haas M. Histology and immunohistology of IgA nephropathy. *J Nephrol.* 2005;18:676–680.
25. van der Boog PJ, van Kooten C, van Seggelen A, et al. An increased polymeric IgA level is not a prognostic marker for progressive IgA nephropathy. *Nephrol Dial Transplant.* 2004;19:2487–2493. <https://doi.org/10.1093/ndt/gfh394>